BULLETIN OF THE POLISH ACADEMY OF SCIENCES
TECHNICAL SCIENCES, Vol. 61, No. 3, 2013
DOI: 10.2478/bpasts-2013-0059

Fractional-order models of the supercapacitors in the form of RC ladder networks

W. MITKOWSKI and P. SKRUCH*

Faculty of Electrical Engineering, Automatics, Computer Science and Biomedical Engineering, Department of Automatics and Biomedical Engineering, AGH University of Science and Technology, 30/B1 A. Mickiewicza Ave., 30-059 Cracow, Poland

Abstract. In the paper, mathematical models of the supercapacitors are investigated. The models are based on electrical circuits in the form of RC ladder networks. The elementary cell of the network may consist of resistances and capacitances that are connected in series or parallel. The dynamic behavior of the circuit is described using fractional-order differential equations and its properties are analyzed. The identification procedure with quadratic performance index is performed in time domain to identify the parameters of the supercapacitor models. The results of numerical simulations are compared with the results measured experimentally in the physical system. In addition, an example from the automotive industry is used for an experimental evaluation of the theoretical analysis and to present a perspective on the applicability of the approach for other industrial projects.

Key words: fractional-order model; electrical ladder network; supercapacitor; identification.

1. Introduction

1.1. Motivation. In recent years there has been a growing attention to studies on ladder networks because they can be employed to model both electrical and nonelectrical systems with distributed parameters. Electric ladder networks can be described as networks formed by numerous repetitions of an elementary cell. The elementary cell may consist of resistors, inductance coils, and capacitors connected in series or in parallel. The properties of the electric ladder network make this model suitable to capture the distributed double-layer capacitance and the distributed electrolyte resistance of the supercapacitors (also called ultracapacitors or electrochemical double-layer capacitors). In addition, the use of fractional-order mathematical models instead of integer-order models can improve the behavior of the model towards the physical system.

1.2. Related work. Various mathematical models have been developed for analyzing the behavior of the supercapacitors. Macroscopic models of the dynamic phenomena occurred during charging process of the double layer in porous electrodes have been developed in [1–3]. Mathematical models of the supercapacitors in the form of electrical circuits have been considered in [4–6]. Fractional-order capacitor models have been also studied in the past. A good source of references to papers in which the fractional capacitor theory is presented can be found in [7] and recently in [8–11]. In general, the problem is not new. Some simple experiments were performed by S. Westerlund and M.J. Curie's in 1889 (see [7, chap. 10.3, p. 278 and the following] and also [8, chap. 7, p. 127 and the following]). The papers [9, 12] cope with a supercapacitor equivalent model where the capacitance is described using fractional-order calculus (see also [11]). The identification of the supercapacitor parameters is performed in frequency domain. Another identification method of the order of the fractional difference is presented in [13]. The method is based on nonlinear programming technique with Marquardt algorithm [14]. Interesting results complemented with experiments can be also found in the PhD thesis [10].

Many authors (e.g., [7, 15–17]) consider the non-integer order systems to describe dynamical behavior of materials and processes over time and frequency scales. There has been also a lot of studies devoted to the analysis of dynamic properties of such systems, that is stability, controllability, reachability, etc. (see e.g., [18–20]).

The properties of electrical ladder network modelled by integer-order differential equations have been also studied in the past. Control problems of linear RL, RC, LC, and RLC electrical circuits are widely discussed in [21–23]. The dynamics and detailed characteristics of nonlinear electrical circuits are considered in [24].

1.3. Organization of the paper. The paper is organized as follows. In the next section, mathematical models of the supercapacitors in the form of equivalent electrical circuits are described. We start with simple RC circuit with a parallel resistor and then extend it to RC transmission line model. Identification method is briefly explained in Sec. 3. Following section presents experimental results. Applications of the supercapacitors are included in Sec. 5. Conclusions are in Sec. 6.

2. Description of the models

2.1. RC circuit with a parallel resistor. A simple supercapacitor circuit model is composed of a capacitance C_{s}, a series R_{s}, and parallel R_{p} resistances. The electric circuit schematic

*e-mail: pawel.skruch@agh.edu.pl

of the model is illustrated in Fig. 1. The resistance R_s models power loses that may result from internal heating occurring during charging and discharging. The resistance R_p models current leakage, and influences long-term energy storage. Simplicity and computational efficiency can be considered as the main advantages of the model.

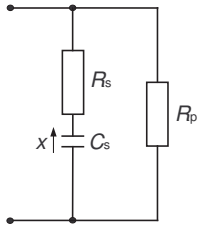

Fig. 1. Electrical circuit model of a supercapacitor in the form of a RC circuit with a parallel resistance

The circuit's dynamic behavior during charging process can be described by the following fractional-order differential equation

$$C_\mathrm{s}R_\mathrm{s}\frac{\mathrm{d}^\alpha x(t)}{\mathrm{d}t^\alpha} = -x(t) + u(t), \qquad x(0) = x_0, \tag{1}$$

where $x(t) \in \mathbb{R}$ is the voltage across the plates of the capacitor C_s, $\alpha \in (0, 1]$ denotes the order of the fractional derivative according to the Caputo definition [7], $x_0 \in \mathbb{R}$ is the given initial condition, $t > 0$. When the power supply is disconnected from the circuit, the discharge process of the supercapacitor will be described by the following equation

$$C_\mathrm{s}(R_\mathrm{s} + R_\mathrm{p})\frac{\mathrm{d}^\alpha x(t)}{\mathrm{d}t^\alpha} = -x(t), \qquad x(0) = x_0. \tag{2}$$

2.2. RC transmission line model. A transmission line model in the form of RC ladder network is presented in Fig. 2. The transmission line model attempts to capture the distributed double-layer capacitance and the distributed electrolyte resistance that extends the depth of the pore.

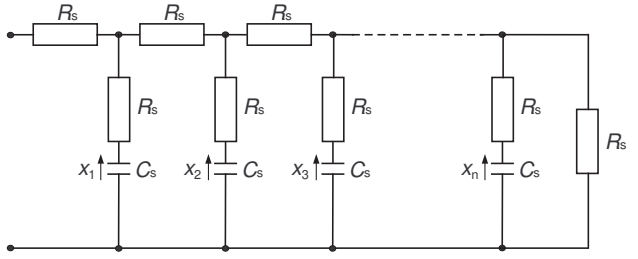

Fig. 2. Electrical circuit model of a supercapacitor in the form of a RC ladder network

The dynamic behavior of the RC ladder network can be described by the following fractional-order differential equations

$$C_\mathrm{s}R_\mathrm{s}\boldsymbol{D}\frac{\mathrm{d}^\alpha \boldsymbol{x}(t)}{\mathrm{d}t^\alpha} = \boldsymbol{A}\boldsymbol{x}(t) + \boldsymbol{B}u(t), \qquad \boldsymbol{x}(0) = \boldsymbol{x}_0, \tag{3}$$

where $\boldsymbol{x}(t) = [x_1(t)\ x_2(t)\ \ldots\ x_n(t)]^\mathrm{T} \in \mathbb{R}^n$, $\boldsymbol{x}_0 \in \mathbb{R}^n$, $u(t) \in \mathbb{R}$, $t > 0$, $\alpha \in (0, 1]$, $t > 0$,

$$\boldsymbol{D} = \begin{bmatrix} 3 & -1 & 0 & \ldots & 0 & 0 & 0 \\ -1 & 3 & -1 & \ldots & 0 & 0 & 0 \\ 0 & -1 & 3 & \ldots & 0 & 0 & 0 \\ \vdots & \vdots & \vdots & \ddots & \vdots & \vdots & \vdots \\ 0 & 0 & 0 & \ldots & -1 & 3 & -1 \\ 0 & 0 & 0 & \ldots & 0 & -1 & 3 \end{bmatrix}_{n\times n}, \tag{4}$$

$$\boldsymbol{A} = \begin{bmatrix} -2 & 1 & 0 & \ldots & 0 & 0 & 0 \\ 1 & -2 & 1 & \ldots & 0 & 0 & 0 \\ 0 & 1 & -2 & \ldots & 0 & 0 & 0 \\ \vdots & \vdots & \vdots & \ddots & \vdots & \vdots & \vdots \\ 0 & 0 & 0 & \ldots & 1 & -2 & 1 \\ 0 & 0 & 0 & \ldots & 0 & 1 & -2 \end{bmatrix}_{n\times n}, \tag{5}$$

$$\boldsymbol{B} = \begin{bmatrix} 1 \\ 0 \\ \vdots \\ 0 \end{bmatrix}_{n\times 1}.$$

Remark 1. We consider an $n \times n$ tridiagonal Jacobi matrix $\boldsymbol{E}(n; b)$ given by the following equality

$$\boldsymbol{E}(n; b) = \begin{bmatrix} b & 1 & 0 & \ldots & 0 \\ 1 & b & 1 & \ldots & 0 \\ 0 & 1 & b & \ldots & 0 \\ \vdots & \vdots & \vdots & \ddots & \vdots \\ 0 & 0 & 0 & \ldots & 0 \end{bmatrix}. \tag{6}$$

The eigenvalues of the $n \times n$ matrix $\boldsymbol{E}(n; b)$ (see [25, p. 215], [26, p. 159], [27, p. 104]; see also [28,29]) are given by

$$s_k(\boldsymbol{E}(n; b)) = b + 2\cos\varphi_k, \quad \varphi_k = k\pi/(n + 1), \quad k = 1, 2, \ldots, n. \tag{7}$$

Let

$$\boldsymbol{P} = \sqrt{\frac{2}{n+1}} \begin{bmatrix} \sin\varphi_1 & \sin 2\varphi_1 & \ldots & \sin n\varphi_1 \\ \sin\varphi_2 & \sin 2\varphi_2 & \ldots & \sin n\varphi_2 \\ \vdots & \vdots & \ddots & \vdots \\ \sin\varphi_n & \sin 2\varphi_n & \ldots & \sin n\varphi_n \end{bmatrix}, \tag{8}$$

where φ_k is given in (7). You can check that $\boldsymbol{P}^2 = \boldsymbol{I}$. Thus $\boldsymbol{P}^{-1} = \boldsymbol{P}$ and $\boldsymbol{P}\boldsymbol{E}(n; b)\boldsymbol{P} = \mathrm{diag}\,(s_1, s_2, \ldots, s_n)$, where s_k is given in (7).

Also note that $\boldsymbol{E}(n; e + g) = \boldsymbol{E}(n; e) + g\boldsymbol{I}$, where $\boldsymbol{I}$ is the identity matrix $n \times n$. Consequently

$$s_k(\boldsymbol{E}(n; e + g)) = e + g + 2\cos\varphi_k. \tag{9}$$

Theorem 1. The system (3) is diagonalizable, that is, the system (3) can be broken down into n scalar systems.

Proof. Let $\boldsymbol{x}(t) = \boldsymbol{P}\boldsymbol{z}(t)$, where $\boldsymbol{P}$ is given in (8), $\det \boldsymbol{P} \neq 0$. In this case $\boldsymbol{P}^{-1} = \boldsymbol{P}$. Thus $\boldsymbol{z}(t) = \boldsymbol{P}\boldsymbol{x}(t)$ and from (3) we

have

$$C_{\mathrm{s}}R_{\mathrm{s}}\boldsymbol{PDP}\frac{\mathrm{d}^{\alpha}\boldsymbol{z}(t)}{\mathrm{d}t^{\alpha}} = \boldsymbol{PAPz}(t) + \boldsymbol{PB}u(t). \tag{10}$$

Notice that $\boldsymbol{D} = -\boldsymbol{E}(n;-3)$, $\boldsymbol{A} = \boldsymbol{E}(n;-2)$ and (see Remark 2)

$$C_{\mathrm{s}}R_{\mathrm{s}}s_k(\boldsymbol{D})\frac{\mathrm{d}^{\alpha}z_k(t)}{\mathrm{d}t^{\alpha}} = s_k(\boldsymbol{A})z_k(t) + \sqrt{\frac{2}{n+1}}\sin\varphi_k u(t), \tag{11}$$

where $k = 1, 2, \ldots, n$ and

$$\begin{aligned} s_k(\boldsymbol{D}) &= 1 + 4\sin^2\frac{\varphi_k}{2} > 0, \\ s_k(\boldsymbol{A}) &= -4\sin^2\frac{\varphi_k}{2} < 0. \end{aligned} \tag{12}$$

Example 1. Consider matrices $\boldsymbol{D}$ and $\boldsymbol{A}$ for $n = 5$. In this case

$$\boldsymbol{P} = \begin{bmatrix} -0.2887 & -0.5000 & 0.5774 & -0.5000 & 0.2887 \\ -0.5000 & -0.5000 & -0.0000 & -0.5000 & -0.5000 \\ -0.5774 & 0.0000 & -0.5774 & -0.0000 & 0.5774 \\ -0.5000 & 0.5000 & -0.0000 & -0.5000 & -0.5000 \\ -0.2887 & 0.5000 & 0.5774 & 0.5000 & 0.2887 \end{bmatrix}, \tag{13}$$

and

$$\boldsymbol{PDP} = \mathrm{diag}\,(1.2679,\ 2.0000,\ 3.0000,\ 4.0000,\ 4.7321), \tag{14}$$

$$\boldsymbol{PAP} = \mathrm{diag}\,(-0.2679,\ -1.0000,\ -2.0000,\ -3.0000,\ -3.7321). \tag{15}$$

From (11) and (12) we have

$$\frac{\mathrm{d}^{\alpha}z_k(t)}{\mathrm{d}t^{\alpha}} = a_k z_k(t) + b_k u(t), \quad k = 1, 2, \ldots, n, \tag{16}$$

where

$$\begin{aligned} a_k &= \frac{4\sin^2\frac{\varphi_k}{2}}{C_{\mathrm{s}}R_{\mathrm{s}}\left(1 + 4\sin^2\frac{\varphi_k}{2}\right)}, \\ b_k &= \frac{\sqrt{\frac{2}{n+1}}\sin\varphi_k}{C_{\mathrm{s}}R_{\mathrm{s}}\left(1 + 4\sin^2\frac{\varphi_k}{2}\right)}. \end{aligned} \tag{17}$$

The function $G(s)$ of the system (16) is given by

$$G(s) = \frac{b_k}{s^{\alpha} - a_k} = \frac{Y_k(s)}{U_k(s)}. \tag{18}$$

Remark 2. For $k = 1, 2, \ldots, n$ each scalar equation (11) or (16) can be solved using the formula given in the works: [11, p. 32], [15, p. 92], see also [17, p. 65, 74].

The unit step response of the system (18) can be expressed as

$$y_k(t) = L^{-1}\{G(s)\} = b_k t^{\alpha} E_{\alpha,\alpha+1}(a_k t^{\alpha}), \tag{19}$$

where $E_{\nu,\gamma}$ is the Mittag-Leffler function in two parameters (see e.g., [7, p. 17])

$$E_{\nu,\gamma}(w) = \sum_{i=0}^{\infty}\frac{w^i}{\Gamma(\nu i + \gamma)}. \tag{20}$$

The gamma function $\Gamma(x)$ is defined by the integral [7, p. 1]

$$\Gamma(x) = \int_0^{\infty} \mathrm{e}^{-t}t^{x-1}\,\mathrm{d}t, \tag{21}$$

which converges in the right half of the complex plane $\mathrm{Re}\,(x) > 0$.

Remark 3. The system (16) is BIBO stable (Bounded Input Bounded Output). This is evident with the stability criterion given, for example, in the work [8, p. 21 and 22].

3. Identification method

Denote by $\boldsymbol{\theta}$ a vector that contains the parameters to be identified. Assume that a vector function $\overline{\boldsymbol{v}_{\mathrm{s}}}(\cdot)$ contains measurement data collected during the experiments, and a vector function $\boldsymbol{v}_{\mathrm{s}}(\cdot)$ represents estimated data calculated during simulations for a given set of the parameters $\boldsymbol{\theta}$. In addition, denote by $\boldsymbol{\epsilon}(\cdot)$ the error function

$$\boldsymbol{\epsilon}(t) = \overline{\boldsymbol{v}_{\mathrm{s}}}(t) - \boldsymbol{v}_{\mathrm{s}}(t) \tag{22}$$

between the experimental and simulated data.

The identification problem is to find a vector $\boldsymbol{\theta} \in \Theta_{\mathrm{ad}}$ that minimizes the quadratic criterion J, that is,

$$\min_{\boldsymbol{\theta}\in\Theta_{\mathrm{ad}}} J, \tag{23}$$

where

$$J = \int_0^{T} \boldsymbol{\epsilon}(\tau)^{\mathrm{T}}\boldsymbol{W}\boldsymbol{\epsilon}(\tau)\,\mathrm{d}\tau, \tag{24}$$

Θ_{ad} stands for the set of admissible parameters, $\boldsymbol{W}^{\mathrm{T}} = \boldsymbol{W}$ is a positive definite weighting matrix, T denotes simulation time.

The problem (23) can be solved efficiently using many optimization algorithms. For example, in [13], nonlinear programming technique with Marquardt algorithm [14] has been successfully used. In this paper, the identification procedure has been implemented in MATLAB® environment using the Nelder-Mead simplex (direct search) method [30]. The fractional continuous-time linear system that is used to model the supercapacitor has been simulated also in MATLAB environment. In the simulation experiment, the system solution expressed by the Mittag-Leffler matrix function has been utilized (see e.g., [31]). The number of samples in sum operation in the calculation of the Mittag-Leffler matrix function has been limited to 150. The measurement data have been obtained using the test bench as presented in Fig. 3.

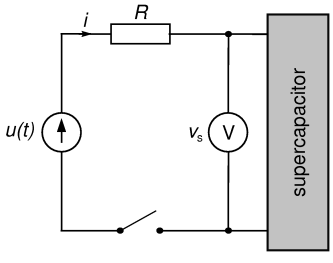

Fig. 3. Schematic diagram of the test bench for identification of the supercapacitor parameters

4. Experimental results

The supercapacitor SAMSON DRE22/2.5 (capacitance 22 F, operating voltage 2.5 V) has been exploited in the experiments.

The parameters $\boldsymbol{\theta} = [\alpha\, R_\mathrm{s}\, R_\mathrm{p}]^\mathrm{T}$ of the model (1), (2) have been determined via a least-squares procedure minimizing the performance index (24) for $\boldsymbol{W} = [1]$. In this case, the voltage $v_\mathrm{s}(t)$ (see Fig. 3) across the terminals of the supercapacitor

$$v_\mathrm{s}(t) = x(t) + R_\mathrm{s}C_\mathrm{s}\frac{\mathrm{d}^\alpha x(t)}{\mathrm{d}t^\alpha} \tag{25}$$

has been compared with the voltage waveform measured experimentally in the physical system. The identified parameters are presented in Table 1. The graphical comparison of the simulated and measured voltage waveforms are illustrated in Fig. 4.

In case of the model (3), the parameters $\boldsymbol{\theta} = [\alpha\, R_\mathrm{s}]^\mathrm{T}$ have been identified for $n = 5$. The voltage measured across the terminals of the supercapacitors can be calculated as follows

$$\begin{aligned} v_\mathrm{s}(t) &= x_1(t) + R_\mathrm{s}C_\mathrm{s}\frac{\mathrm{d}^\alpha x_1(t)}{\mathrm{d}t^\alpha} \\ &+\frac{R_\mathrm{s}}{R+R_\mathrm{s}}\left(u(t) - x_1(t) - R_\mathrm{s}C_\mathrm{s}\frac{\mathrm{d}^\alpha x_1(t)}{\mathrm{d}t^\alpha}\right). \end{aligned} \tag{26}$$

Table 1 contains the parameters that have been obtained via a least-squares identification procedure where the weighting matrix $\boldsymbol{W} = \boldsymbol{I}$ has been chosen as identity matrix. Figure 5 illustrates graphically the effect of the identification procedure.

Table 1
Results of the numerical identification of the parameters for the supercapacitor circuit models

Model	C_s [F]	R_s [Ω]	R_p [Ω]	α
RC circuit with parallel resistor	22	0.03	0.19	0.88
RC transmission line for $n = 5$	22	0.01	–	0.74

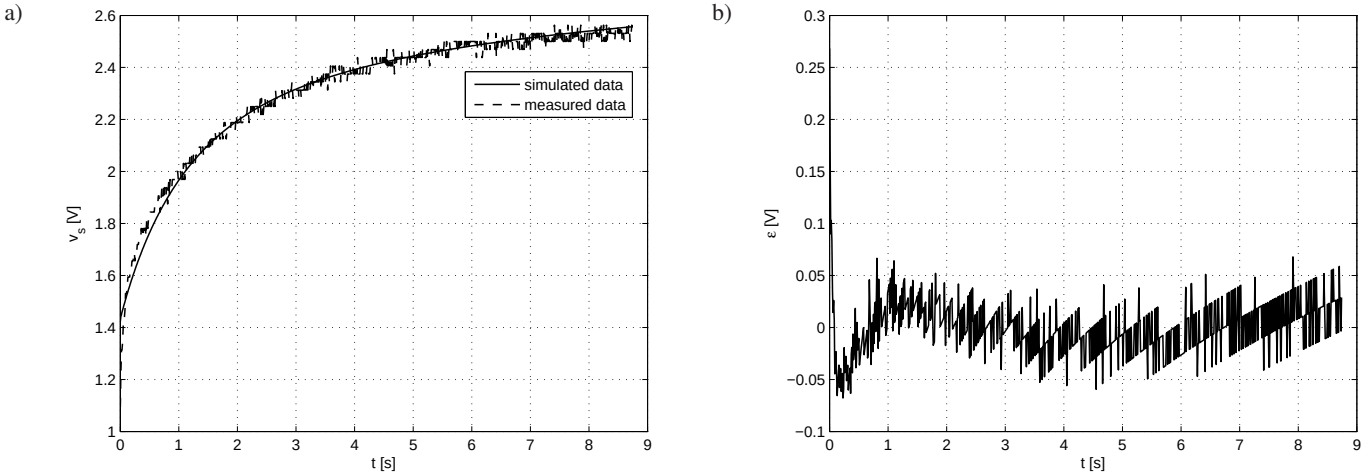

Fig. 4. a) Comparison of the simulated (solid line) and measured (dotted line) voltage waveforms for the 22F/2.5V supercapacitor; b) difference ϵ between simulated and measured values. The simulation data are based on the model presented in Fig. 1

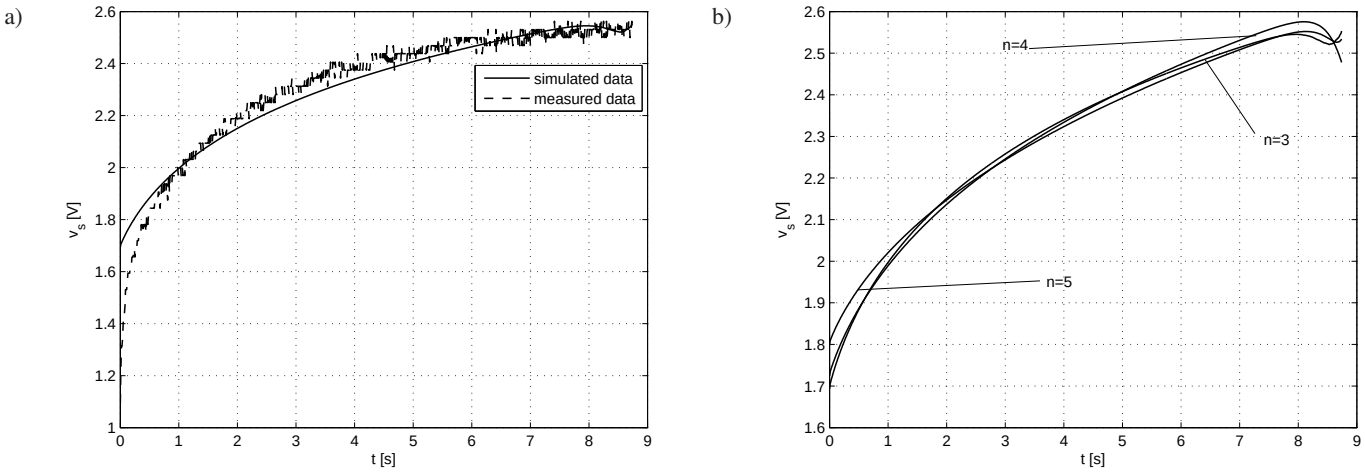

Fig. 5. (a) Comparison of the simulated (solid line) and measured (dotted line) voltage waveforms for the 22F/2.5V supercapacitor; b) comparison of the simulated voltage waveforms for different $n \in \{3, 4, 5\}$. The simulation data are based on the model presented in Fig. 2 for $n = 5$

5. Applications

Supercapacitors are primarily used for energy storage purposes in a variety of commercial applications. They can act as short-term backup supplies to retain data in digital components with memory in case of a short interruption in the power supply. The supercapacitors offer long performance lifetime and therefore do not need to be replaced regularly as it is in case of batteries. Using a supercapacitor in combination with a battery can relieve the battery of the most severe load demands by meeting the peak power requirements, and allowing the battery to supply the average load. The reduction in pulsed current drawn from the battery can result in an extended battery lifetime in portable electronic devices such as laptops and mobile phones.

The ability of the supercapacitors to deliver high electrical performance can resolve the limitation of lead-acid and lithium-ion batteries in the automotive industry [32]. This issue is especially challenging in hybrid and electric vehicles that are getting more and more popular as well as in vehicles equipped with automated Start & Stop systems. The use of the supercapacitors can support cold cranking condition and therefore extend battery life. The support of warm cranking condition in Start & Stop systems can improve the fuel efficiency. The supercapacitors find also applications in KERS (Kinetic Energy Recovery System) systems in regenerative energy capture during braking and coasting. The promising application areas are distributed power systems where the supercapacitors can play an important role in reducing wiring size, weight, and consequently cost.

Consider a battery model that is based on a simple electrical circuit shown in Fig. 6. The circuit consists of a bulk capacitance $C_{\rm cb}$, a surface capacitance $C_{\rm cs}$, an internal resistance $R_{\rm i}$, and a polarization resistance $R_{\rm t}$. The bulk capacitor characterizes the ability of the battery to store charge and the surface capacitor represents battery diffusion effects. The voltages across the bulk capacitor and the surface capacitor are denoted by $V_{\rm cb}$ and $V_{\rm cs}$, respectively. The current and voltage observed at the terminals of the battery are represented in the circuit by I and U, respectively. The current I is taken as positive in case of charging and negative otherwise.

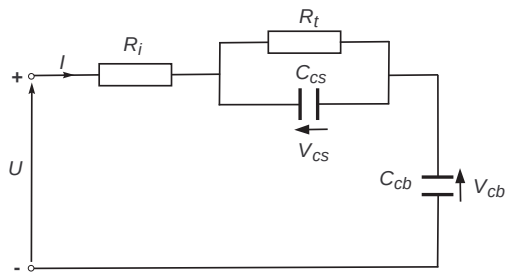

Fig. 6. Electrical circuit model of a battery

The dynamic behavior of the model in Fig. 6 can be governed by the following equations:

$$\frac{{\rm d}^{\alpha}V_{\rm cb}(t)}{{\rm d}t^{\alpha}} = \frac{1}{C_{\rm cb}}I(t), \tag{27}$$

$$\frac{{\rm d}^{\alpha}V_{\rm cs}(t)}{{\rm d}t^{\alpha}} = -\frac{1}{R_{\rm t}C_{\rm cs}}V_{\rm cs}(t) + \frac{1}{C_{\rm cs}}I(t), \tag{28}$$

$$U(t) = V_{\rm cs}(t) + V_{\rm cb}(t) + R_{\rm i}I(t). \tag{29}$$

By defining the following state variables

$$x_1(t) = V_{\rm cb}(t), \qquad x_2(t) = V_{\rm cs}(t), \tag{30}$$

and denoting the input and output as

$$u(t) = I(t), \qquad y(t) = U(t), \tag{31}$$

we can formulate a fractional-order state space model of the battery

$$\frac{{\rm d}^{\alpha}\boldsymbol{x}(t)}{{\rm d}t^{\alpha}} = \boldsymbol{A}\boldsymbol{x}(t) + \boldsymbol{B}u(t), \tag{32}$$

$$y(t) = \boldsymbol{C}\boldsymbol{x}(t) + Du(t), \tag{33}$$

where $\boldsymbol{x}(t) = [x_1(t)\ x_2(t)]^{\rm T}$, $\alpha \in (0, 1]$, $t > 0$ and

$$\boldsymbol{A} = \begin{bmatrix} 0 & 0 \\ 0 & -\dfrac{1}{R_{\rm t}C_{\rm cs}} \end{bmatrix}, \qquad \boldsymbol{B} = \begin{bmatrix} C_{\rm cb}^{-1} \\ C_{\rm cs}^{-1} \end{bmatrix}, \qquad \boldsymbol{C} = \begin{bmatrix} 1 & 1 \end{bmatrix}, \qquad D = \begin{bmatrix} R_{\rm i} \end{bmatrix}. \tag{34}$$

Power management applications in the automotive electronics systems are subject to wide input voltage fluctuations resulting from load dump, jump start, and cold-cranking conditions. A load dump occurs when the battery is disconnected while the engine and the alternator are running. A jump start or boost occurs when a second battery (often from another vehicle) is temporarily connected to recharge the dead battery of the disabled vehicle. A cold-cranking condition occurs during the startup of a vehicle engine. In such situation the battery supplies a large current to the electric starter motor. At the same time the battery voltage drops dramatically even below 5 V what could cause reset of many electronic devices in the vehicle. Figure 7 shows a typical cold-cranking profile.

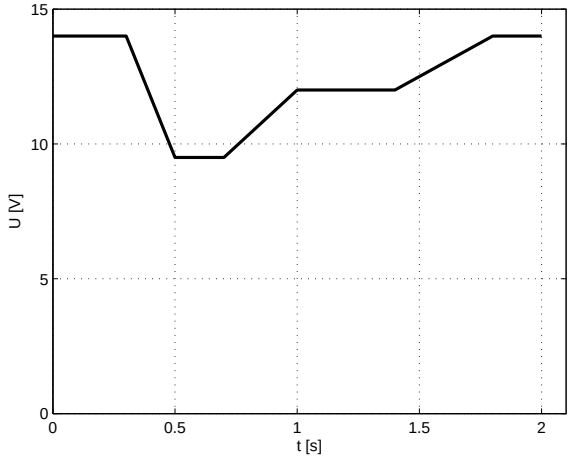

Fig. 7. An example of typical cold-cranking profile

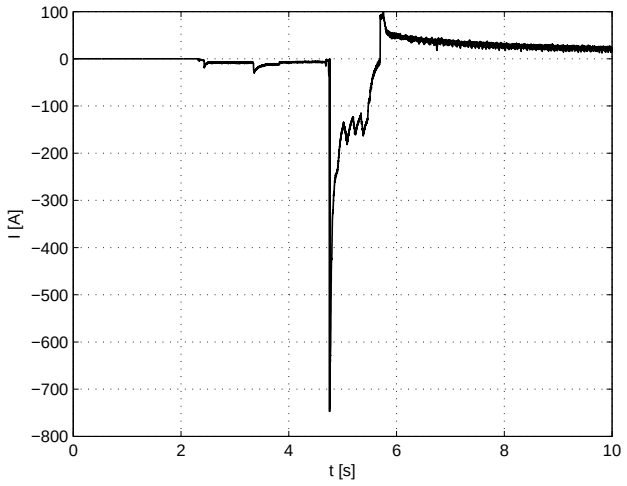

Fig. 8. Current waveform during vehicle cranking (data collected from a real vehicle)

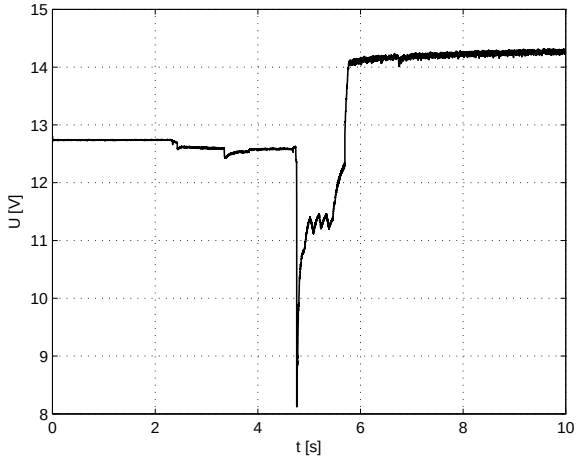

Fig. 9. Voltage waveform during vehicle cranking (data collected from a real vehicle)

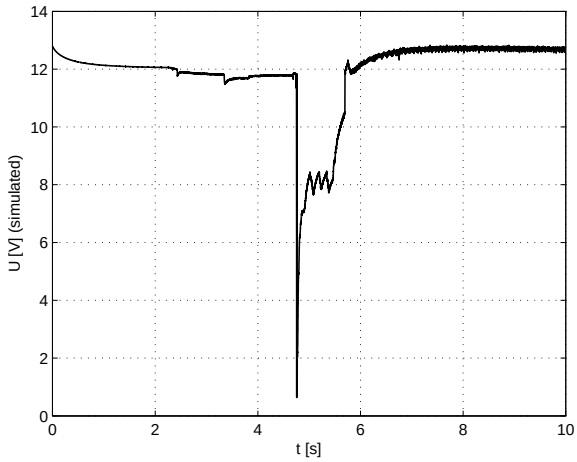

Fig. 10. Simulated voltage waveform during vehicle cranking (data collected from the battery model (32), (33))

Table 2
Parameters of the battery model

Parameter	Value	Unit
C_{cb}	50000	F
C_{cs}	30	F
R_{i}	0.015	Ohm
R_{t}	0.015	Ohm
α	0.8	–

The voltage (Fig. 9) and current (Fig. 8) waveforms have been measured during crank operation. These data can be used to identify the parameters of the battery model (32), (33) (see Table 2). Simulated voltage waveform is presented in Fig. 10.

6. Conclusions

Fractional-order models can be successfully utilized to describe mathematically the dynamic behavior of the supercapacitors. In the paper, equivalent electrical circuit models in the form of RC ladder networks have been used to verify the hypothesis. The comparison of simulation and experimental data has shown the effectiveness of the proposed modelling methodology.

Acknowledgements. This work was supported by the National Science Centre (Poland) – project No N N514 644440.

REFERENCES

[1] A.M. Johnson and J. Newman, "Desalting by means of porous carbon electrodes", *J. Electrochemical Society* 118 (3), 510—517 (1971).

[2] F. Posey and T. Morozumi, "Theory of potentiostatic and galvanostatic charging of the double layer in porous electrodes", *J. Electrochemical Society* 113 (2), 176–184 (1966).

[3] V. Srinivasan and J.W. Weidner, "Mathematical modeling of electrochemical capacitors", *J. Electrochemical Society* 146 (5), 1650–1658 (1999).

[4] S. Buller, E. Karden, D. Kok, and R.W. De Doncker, "Modeling the dynamic behavior of supercapacitors using impedance spectroscopy", *IEEE Trans. on Industry Applications* 38 (6), 1622–1626 (2002).

[5] R. Setlak and M. Fice, "Modeling of electric energy storages for electric and hybrid vehicles", *Problem Notebooks – Electrical Machines* 2 (90), 145–150 (2011).

[6] L. Shi and M.L. Crow, "Comparison of ultracapacitor electric circuit models", *Proc. IEEE Power and Energy Society General Meeting – Conversion and Delivery of Electrical Energy in the 21st Century* 1, 1–6 (2008).

[7] I. Podlubny, *Fractional Differential Equations*, Holt, Rinehart, and Winston, San Diego, 1999.

[8] R. Caponetto, G. Dongola, L. Fortuna, and I. Petras, *Fractional Order Systems: Modeling and Control Applications*, World Scientific, New Jersey, 2010.

[9] A. Dzielinski, G. Sarwas, and D. Sierociuk, "Comparison and validation of integer and fractional order ultracapacitor models", *Advances in Difference Equations* 2011 (1), 11–23 (2011).

[10] G. Sarwas, "Modelling and control of systems with ultracapacitors using fractional order calculus", *PhD Thesis*, Warsaw University of Technology, Warsaw, 2012.

[11] D. Sierociuk, "Control and estimation of the discrete fractional-order models described in state space", *PhD Thesis*, Warsaw University of Technology, Warsaw, 2007, (in Polish).
[12] A. Dzielinski and D. Sierociuk, "Ultracapacitor modelling and control using discrete fractional order state-space model", *Acta Montanistica Slovaca* 113 (1), 136–145 (2008).
[13] W. Mitkowski and A. Obraczka, "Simple identyfication of fractional differential equation", *Solid State Phenomena* 180, 331–338 (2012).
[14] D.W. Marquardt, "An algorithm for least-squares estimation of nonlinear parameters", *J. Society for Industrial and Applied Mathematics* 11 (2), 431–441 (1963).
[15] T. Kaczorek, "Positive fractional linear systems", *Measurements, Automatics, Robotics* 15 (2), 91–112 (2011).
[16] I. Pan and S. Das, *Intelligent Fractional Order Systems and Control. An Introduction. Studies in Computational Intelligence, 438*, Springer, Berlin, 2013.
[17] M. Weilbeer, "Efficient numerical methods for fractional differential equations and their analytical background", *PhD Thesis*, Technical University Braunschweig, Braunschweig 2005.
[18] M. Buslowicz, "Stability of state-space models of linear continuous-time fractional order systems", *Acta Mechanica et Automatica* 5 (2), 15–22 (2011).
[19] A. Dzielinski and D. Sierociuk, "Stability of discrete fractional order state-space systems", *J. Vibration and Control* 14 (9–10), 1543–1556 (2008).
[20] T. Kaczorek, "Reachability and controllability to zero of cone fractional linear systems", *Archives of Control Sciences* 17 (3), 357–367 (2007).
[21] W. Mitkowski, *Stabilization of Dynamic Systems*, WNT, Warsaw, 1991.
[22] W. Mitkowski, "Dynamic feedback in LC ladder network", *Bull. Pol. Ac.: Tech.* 51 (2), 173–180 (2003).
[23] W. Mitkowski, "Stabilization of LC ladder network", *Bull. Pol. Ac.: Tech.* 52 (2), 109–114 (2004).
[24] S. Mitkowski, *Nonlinear Electric Circuits*, AGH, Cracow, 1999.
[25] R. Bellman, *Introduction to Matrix Analysis*, McGraw-Hill, New York, 1960.
[26] V.P. Ilin and Yu.I. Kuznyetsow, *Tridiagonal Matrices and their Applications*, Science, Moscow, 1985, (in Russian).
[27] P. Lancaster, *Theory of Matrix*, Academic Press, New York, 1969.
[28] W. Mitkowski, "Uniform ladder networks with linear feedback", *Archives of Electrical Engineering* 36, 7–18 (1987).
[29] W. Mitkowski, "Synthesis of RC-ladder network", *Bull. Pol. Ac.: Tech.* 42 (1), 33–37 (1994).
[30] J.A. Nelder and R. Mead, "A simplex method for function minimization", *Computer J.* 7 (4), 308–313 (1965).
[31] T. Kaczorek, "Reachability of cone fractional continuous-time linear systems", *Int. J. Applied Mathematics and Computer Science* 19 (1), 89–93 (2009).
[32] A. Burke, "Ultracapacitor technologies and application in hybrid and electric vehicles", *Int. J. Energy Research* 34 (2), 133–151 (2010).